Journal of Theoretical and Applied Information Technology
30th November 2016. Vol.93. No.2

ISSN: 1992-8645 www.jatit.org E-ISSN: 1817-3195

TEXTURE CLASSIFICATION BASED ON STATISTICAL PROPERTIES OF LOCAL UNITS

[1]M. SRINIVASA RAO, [2]V.VIJAYA KUMAR, [3]MHM KRISHNA PRASAD
[1]Associate Professor, Dept of CSE, Sri Vasavi Institute of Engineering & Technology, pedana, Andhrapradesh, India
[2] Professor, Dean and Director for CACR, Anurag Group of Institutions (Autonomous), Hyderabad, Telangana, India
[3]Professor of the CSE, University College of Engineering, Kakinada (Autonomous), JNTUK, Andhra Pradesh, India

E-mail: [1] srinu.mekala@gmail.com, [2] vakula_vijay@yahoo.com, [3]krishnaprasad.mhm@gmail.com

ABSTRACT

One of the important and crucial tasks of image analysis is to derive significant features of the images. The gray level co-occurrence matrix (GLCM) and its features derived by Haralick are widely known for texture classification. The main disadvantage of GLCM is its high dimensionality when applied on the grey level image. The local features derived from local binary pattern (LBP) have shown significant results in various image and video processing applications. The present paper derived the fundamental rotational invariant local features from LBP in the form of uniform LBP (ULBP) and treated all non-uniform LBP (NULBP) as miscellaneous. After encoding the texture into ULBP coded texture the present paper derived GLCM features and performed texture classification rate, mean absolute error and root mean square error on Brodtaz textures using various machine learning classifiers. The proposed uniform local binary pattern matrix (ULBPM) is compared with GLCM method, cross diagonal texture unit matrix (CDTM) and texture spectrum (TS) methods. The results indicate high performance of the proposed method over the existing methods.

Keywords: *Local Features, Uniform Local Binary Pattern (ULBP), Texture Classification, Graylevel Co-Occurrence Matrix***.**

1. INTRODUCTION

Texture is a primary feature of object surfaces and is widely used in object surface recognition and description. Texture classification plays a crucial role in texture analysis, and it is an active research area in pattern recognition and image processing. Designing a robust algorithm that deals with rotational invariance and illumination changes is still a challenging task in texture classification.

Texture analysis methods are mostly divided in to two different methods: statistical or stochastic and structural methods. The methods based on statistical texture features, extracts them from the statistical distribution of grey levels at particular positions relative to each other in the image. The statistical methods are divided into first-order, second-order and higher-order statistics based on the grey levels at each co-ordinate position. The conventional statistical methods to texture classification such as grey level co-occurrence matrices (GLCM) [8], second order statistics, run length matrix [39, 49] and gaussian markov random fields (GMRF) [11]are based on second order statistics. The approaches that are based on texture primitives or texels (micro-texture), their hierarchy of spatial arrangements with neighboring pixels (macro-texture) and placement rules are known as structural approaches [12].The structural approach treats a texture as the repetition of one or more primitive attributes with a certain rule of placement. The well-known examples of structural approaches are traditional Fourier spectrum analysis [24], the theory of textons [13, 15]. The effect of pattern trends (complex and simple patterns) in texture classification is also studied in the literature [41, 45, 46]. The crucial and most interesting problem of texture classification is how to derive accurate texture features (local, global, structural, statistical or hybrid) that classifies the particular set of textures that are considered.

One of the well-known and widely used structural approach known as LBP operator was introduced by Ojala et.al [27]. The LBP is popular in various applications because it holds the significant local attributes efficiently and more over

Journal of Theoretical and Applied Information Technology
30th November 2016. Vol.93. No.2

ISSN: 1992-8645 www.jatit.org E-ISSN: 1817-3195

it is a grey scale invariant, simple to implement and understand, and robust. The approaches based on LBP are widely studied and used in texture analysis and classification [18, 22, 23, 28], face detection and recognition [3, 4, 6], image retrieval [1, 38, 40], etc. The other integrated methods that are based on LBP model are [5, 16, 17, 25, 26, 43]. The LBP is initially derived on a 3 x 3 neighborhood with 8 neighbors and later it is extended in to different forms i.e. ULBP [28], multi resolution LBP [27]. LBP is sensitive to noise, image rotation and fails in representing global textural information. The CLBP [50] is derived based on three components the central pixel descriptor, the sign descriptor and the magnitude descriptor and it is aimed to preserve additional information. The dominant LBP (DLBP) [33], prominent LBP (PLBP) [44] reduced the overall dimension of LBP codes by discarding some patterns that have fewer occurrences and treated them as miscellaneous. Researchers also integrated LBP with co-occurrence features [9, 42, 47]. To overcome the random and quantized noise in LBP, Local ternary patterns are introduced [48]. The LTP divides the local neighborhood in to ternary patterns {-1,0,1} by using a threshold and this makes them as significantly more distinctive. However the ternary pattern mechanism of LTP is not fully explored because finally they are split in to binary patterns only. Local quantized patterns (LQP) [32] encoded the binary/ternary pattern using a clustering scheme to reduce the feature dimension. Local color vector binary pattern (LCVBP) [31] is developed for color applications. Recently local n-ary pattern is introduced to overcome this [34] and it is later extended by Local *N*-Ary Pattern. This resulted a good classification.

The rest of the paper is organized as follows. Section two briefly introduces the concept of LBP. The section three presents the methodology. |The section four presents' experimental results and in section five conclusions are drawn.

2. RELATED WORK

2.1 Introduction to LBP

Initially LBP was measured on a 3x3 local neighborhood over a central pixel. The LBP operator assigns a binary value to the neighboring pixel based on a threshold usually the grey level value of the central pixel. The nine pixel elements of a 3×3 circular neighborhood can be represented as, L = {l_c, l_0, l_1…l_7}, where l_c and l_i (0≤i≤7) represents the intensity values of the central and neighboring pixels. The neighboring pixels l_i (0≤i≤7) are converted in to binary pattern elements using equation 1.

$$b_i = \begin{cases} 0 \ \Delta l_i \ \geq 0 \\ 1 \ \Delta \ l_i \ < 0 \end{cases} \quad (1)$$

where $\Delta l_i = l_i - l_c$.

Using these binary pattern elements, a unique LBP code is derived on the neighborhood as given in equation 2 and the central pixel value is replaced by the derived LBP code value. This LBP code defines the local micro texture information around the l_c.

$$LBP_{P,R} = \sum_{i=0}^{i=7} b_i \ x \ 2^i \quad (2)$$

Where p represents the number of neighboring pixels and R is the radius of the neighborhood. The combination of all the eight neighboring elements of the basic LBP [27] results in 2^8 = 256 ranging from 0 to 255 possible local binary patterns (LBP). There is no unique way to label the coefficients and ordering the 256 LBP codes on a 3×3 neighborhood. The Fig. 1 illustrates the operation of basic local binary pattern. Later LBP are derived in various combinations of (P,R) i.e. (8,1),(16,1), (8,2), (16,2) etc..

73	35	55
22	**40**	25
57	20	11

(a)

1	0	1
0		0
1	0	0

(b)

2^0	2^1	2^2
2^7		2^3
2^6	2^5	2^4

(c)

1	0	4
0		0
64	0	0

(d)

Fig. 1: Operation of basic Local Binary Pattern (a) Sample Gray level 3x3 Neighborhood (b) Conversion of gray level 3x3 neighborhood into Binary Neighborhood (c) Representation of Binary Weights(d) Representation of Values with Binary Weights.

The binary values of Fig. 1 (b) are multiplied by their corresponding weights as shown by Fig. 1 (c) and the sum of these results a LBP code in this case

ISSN: 1992-8645 www.jatit.org E-ISSN: 1817-3195

it is 69. The central pixel 40 is replaced by 69. In this way a new LBP image is constructed by replacing the central value with the corresponding LBP codes.

3. PROPOSED METHOD

The algorithm for the present work is given below.

Algorithm:

Step 1: Conversion of colour image into grey level image using RGB colour space.

Step 2: Derivation of local binary pattern on each 3x3 neighborhood.

Step 3: Formation of ULBP matrix (ULBPM): If the LBP forms an ULBP then assign the ULBP index code to the central pixel (uniform index starts from 1 to 58). Otherwise replace the central pixel with an index code of zero (The index code zero is assigned to all NULBPs)

Step 4: Derivation of GLCM features on the ULBPM.

Step 5: Compute texture classification, mean absolute error and root mean squared error rates using various machine learning classifiers.

3.1. Derivation of ULBPM

After a careful study on the patterns of LBP, it is found that only some kind of patterns are occurring dominantly in texture windows and they are named as Uniform LBP(ULBP) [22, 23] and treated as fundamental unit of textures. The ULBPS reduced lot of complexity because it eliminated the process of considering the other kind of patterns for any applications. A pattern is considered 'uniform' (U) if the number of transitions in the sequence between 0 and 1 is less than or equal to two. The kinds of pattern that are having at most two one-to-zero or zero-to-one transitions in the circular binary code generated by LBP are called ULBP. For example, the LBP codes 0 and 255 derive a U value of 0. The patterns 11000000, 00111000, 011110000, 00011111, 01111110 and 11111110 derives a U value of 2.The total number of distinct ULBPs will be P× (P-1) +2 (i.e., 58 of 3×3 neighborhood) of the 2^P un-rotated patterns. It implies there will be 198 NULBPs on a 3x3 window and the ULBP approach treats NULBPs as miscellaneous. This will reduce lot of dimensionality without losing any texture content.

Many investigators [10, 20, 36, 37] considered only ULBPs for their investigations because of the following reasons. a) ULBPs are statistically more significant and there is a need to estimate more reliably and accurately the occurrence probabilities of ULBPs. b) Most LBPs in natural images, textures and human faces are uniform patterns [21, 35]. For example LBP_{u2} 8,1 accounts more than 90% in texture images [21] and LBP_{u2} 8,2 accounts 90.6% in facial images [10]. c) In contrast NULBP's are statistically in significant and they occupy only small portion. In the literature the non-uniform patterns are grouped into one label to suppress noise and by this number of patterns are reduced considerably. The present paper transformed the given texture image in to ULBP coded image with 59 distinct values ranging from 0 to 58 (the index value zero is given to all NULBPS and the index values 1 to 58 are given to ULBP codes). The process of transforming an image of 5 x 5 neighborhood in to ULBPM is shown in Fig.2.

21	35	16	45	56
12	56	85	46	89
54	16	26	35	64
23	15	19	68	45
54	16	39	60	85

(a) Original image neighbourhood

8	0	156
222	31	63
255	62	16

(b)LBP coded image

8	1	0
0	16	22
58	21	12

(c) ULBP coded image

Fig.2: Transformation process of ULBP coded image.

Journal of Theoretical and Applied Information Technology
30th November 2016. Vol.93. No.2

ISSN: 1992-8645 www.jatit.org E-ISSN: 1817-3195

3.2 Grey Level Co-Occurrence Matrix (GLCM) Features

Haralick et al. [11] introduced a second order statistical method "grey level co-occurrence matrix (GLCM)" for texture analysis**.** The GLCM has become one of the standard and benchmark methods for texture analysis. The GLCM characterize textures based on overall or average spatial relationship between grey tones in an image [30]. The size of the GLCM depends on the number of grey levels or intensity levels of an image but not on the dimensions of the image. An image with a size of p x q and with grey levels ranging from 0 to g-1, will derive a GLCM of size g x g. To reduce the dimensionality the original image will be usually quantized. The texture analysis result mainly depends on the quantized process. The quantized method should hold the image attributes significantly and precisely, this will only results a good classification. Let us assume an image G is quantized to N_g number of grey levels. Then, GLCM is evaluated from a grey level image G by scanning the intensity of each and every pixel and its neighbor, defined by displacement d and angle ø. This can have values 1, 2, 3…n whereas an angle, ø is limited 0°, 45°, 90° and 135°. This results a GLCM P(i,j|d,ø) with a joint probability density function P for each element in co-occurrence matrix. Haralick derived 13 features [11] on GLCM and they are given in below. These features are widely used in image analysis, classification, retrieval, interpretation and other applications and they have become the bench mark and the present ULBM derives those features.

$$P_x(i) = \sum_{j=0}^{G-1} P(i,j)$$

$$P_y(j) = \sum_{i=0}^{G-1} P(i,j)$$

$$\mu_x = \sum_{i=0}^{G-1} i \sum_{j=0}^{G-1} P(i,j) = \sum_{i=0}^{G-1} iP_x(i)$$

$$\mu_y = \sum_{i=0}^{G-1} \sum_{j=0}^{G-1} jP(i,j) = \sum_{j=0}^{G-1} jP_x(j)$$

$$\sigma^2{}_x = \sum_{i=0}^{G-1} (i-\mu_x)^2 \sum_{j=0}^{G-1} P(i,j) = \sum_{i=0}^{G-1} \left(P_x(i) - \mu_x(i)\right)^2$$

$$\sigma^2{}_y = \sum_{j=0}^{G-1} \left(i-\mu_y\right)^2 \sum_{i=0}^{G-1} P(i,j) = \sum_{j=0}^{G-1} \left(P_y(j) - \mu_x(j)\right)^2$$

and

$$P_{x+y}(k) = \sum_{i=0}^{G-1} \sum_{j=0}^{G-1} P(i,j) \; i+j=k$$

for k=0, 1, 2, 3…,2(G-1).

$$P_{x-y}(k) = \sum_{i=0}^{G-1} \sum_{j=0}^{G-1} P(i,j) \;\; |i-j| = k$$

for k=0, 1, 2, 3…,(G-1).

where G is the number of grey levels used. μ is the mean value of P. μ_x, μ_y, σ_x and σ_y are the means and standard deviations of Px, Py. Px(i) is ith entry in the marginal-probability matrix obtained by summing the rows of P(i, j).

1. Homogeniety or Angular Second Moment (ASM):

$$ASM = \sum_{i=0}^{G-1} \sum_{j=0}^{G-1} \{P(i,j)\}^2 \quad (3)$$

ASM is a measure of homogeneity of an image. A homogeneous scene will contain only a few grey levels, giving a GLCM with only a few but relatively high values of P (i, j). Thus, the sum of squares will be high.

2. Energy :

$$Energy = \sum_{i,j} P(i,j)^2 \quad (4)$$

3. Local Homogeneity, Inverse Difference Moment (IDM)

$$IDM = \sum_{i=0}^{G-1} \sum_{j=0}^{G-1} \frac{1}{1+(i-j)^2} P(i,j) \quad (5)$$

ISSN: 1992-8645 www.jatit.org E-ISSN: 1817-3195

IDM is also influenced by the homogeneity of the image. Because of the weighting factor (1+(i −j)2)−1 IDM will get small contributions from inhomogeneous areas (i != j). The result is a low IDM value for inhomogeneous images, and a relatively higher value for homogeneous images.

4. Contrast :

$$\text{Contrast} = \sum_{n=0}^{G-1} n^2 \left\{\sum_{i=1}^{G}\sum_{j=1}^{G} P(i,j)\right\}, |i-j| = n \quad (6)$$

This measure of contrast or local intensity variation will favor contributions from P (i, j) away from the diagonal, i.e. i ! = j.

5. Correlation :

$$\text{Correlation} = \sum_{i=0}^{G-1}\sum_{j=0}^{G-1} \frac{\{iXj\}XP(i,j)-\{\mu_x X\mu_y\}}{\sigma_x X\sigma_y} \quad (7)$$

Correlation is a measure of grey level linear dependence between the pixels at the specified positions relative to each other.

6. Entropy :

$$\text{Entropy} = -\sum_{i=0}^{G-1}\sum_{j=0}^{G-1} P(i,j)X\log(P(i,j)) \quad (8)$$

Inhomogeneous scenes have low first order entropy, while a homogeneous scene has high entropy.

7. Sum of Squares, Variance:

$$\text{Variance} = \sum_{i=0}^{G-1}\sum_{j=0}^{G-1}(i-\mu)^2 P(i,j) \quad (9)$$

This feature puts relatively high weights on the elements that differ from the average value of P(i, j).

8. Sum of Average :

$$\text{Average} = \sum_{i=0}^{2G-1} iP_{x+y}(i) \quad (10)$$

9. Sum Entropy(SENT) :

$$\text{SENT} = -\sum_{i=0}^{2G-2} P_{x+y}(i)\log\left(P_{x+y}(i)\right) \quad (11)$$

10. Difference Entropy(DENT):

$$\text{DENT} = -\sum_{i=0}^{G-1} P_{x+y}(i)\log\left(P_{x+y}(i)\right) \quad (12)$$

11. Inertia :

$$\text{Inertia} = \sum_{i=0}^{G-1}\sum_{j=0}^{G-1}\{i-j\}^2 XP(i,j) \quad (13)$$

12. Cluster Shade :

$$\text{Shade} = \sum_{i=0}^{G-1}\sum_{j=0}^{G-1}\{i+j-\mu_x-\mu_y\}^3 XP(i,j) \quad (14)$$

13. Cluster Prominence:

$$\text{Prom} = \sum_{i=0}^{G-1}\sum_{j=0}^{G-1}\{i+j-\mu_x-\mu_y\}^4 XP(i,j) \quad (15)$$

4. RESULTS AND DISCUSSIONS

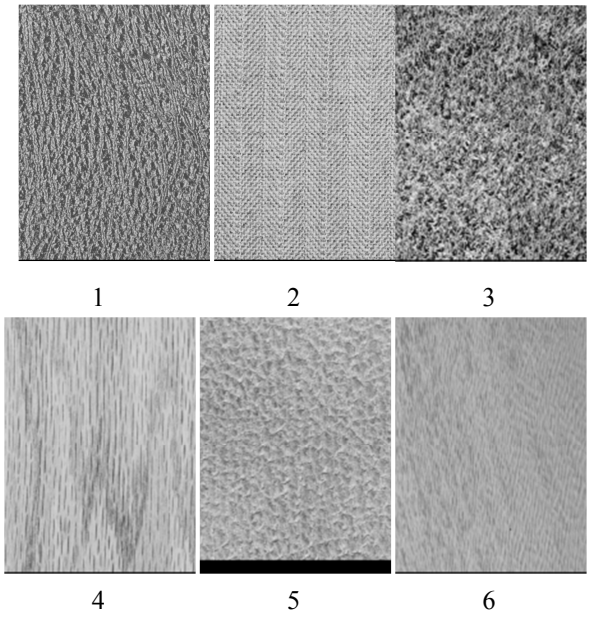

Fig.3: Broadtaz Texture Images.

To examine the effectiveness the present paper carried out experiments on Brodatz [29] textures. The proposed ULBPM is compared with Cross diagonal texture matrix (CDTM) [2], GLCM [14] and texture spectrum (TS) approach [19] This paper selected six different texture classes of images from the Brodtaz database [29], each with a resolution or size of 512 x 512 pixels. They are the images of 1) pressed cork 3) herringbone weave 3) grass lawn 4) wood grain 5) pig skin 6) water (Fig.3). Each texture image is sub divided in to non-overlapped sub images of size 64 x 64 i.e. 64 non overlapped sub image textures. Four textures of each category are considered for experimental sake, out of these

ISSN: 1992-8645 www.jatit.org E-ISSN: 1817-3195

three textures, i.e. 192 sub image textures, from each category are considered for training data base. And 64 sub image textures of the same category are considered for test data base. This paper used 47 textural features in classifying Broadtaz textures. Out of these 13 features on GLCM of original texture image, 8 features of TS, 13 textural features on CDTM and 13 textural features on proposed ULBPM. The present paper measured texture classification rate, mean absolute error and root mean squared error using machine learning classifiers like 1)Multi perceptron, 2) Naïvebayes, 3)J48 and 4) lbk.

Method 1: in this the present paper evaluated the 13 GLCM features on the original image using 0^o, 45^o, 90^o and 135^o degrees and performed the classification using the above mentioned classifiers. The average classification rate is mentioned in the tables.

Method 2: The paper evaluated the eight [7] TS features on the texture images and performed the classification and they are 1) Black-white symmetry (BWS), 2) Geometric symmetry (GS) and 3) Degree of direction (DD). The other orientation features derived on TS are 4) micro-horizontal structures (MHS), 5) Micro-vertical structures (MVS), 6) Micro-first diagonal structures (MDS1), 7) Micro-second diagonal structures (MDS2) and 8) Central symmetry.

Method 3: This paper evaluated the 13 GLCM features on CDTM [2] with different orientations and the average classification rate using different classifiers is listed in the tables. The size of GLCM on CDTM is 81x81.

Proposed ULBPM (method 4): In this the present paper initially quantized the image in to ULBP coded image. The size of ULBPM is 0 to 58 x 0 to 58. Then Haralick features are evaluated using 0^o, 45^o, 90^o and 135^o degrees and average classification rate is listed. .

The features from the three existing methods and the proposed ULBPM are evaluated on all training data set of images and given to various machine learning classifiers and the classification rate, mean absolute error rate and root mean squared error rate are listed in tables. The method2 on the texture images resulted a poor classification rate on all classifiers and it has exhibited an average classification rate of 53.63, a high mean absolute error and root mean squared error rate of 0.69 and 0.68 respectively (average of all classifiers). However they have a high classification rate by using Ibk classifier.

The GLCM features on the original textures achieved an average texture classification rate of 62.58%, mean absolute error of 0.39 and root mean squared error of 0.51 (average of all classifiers). These features on different classifiers have not improved the overall classification rate. CDTM approach, using 13 GLCM features, with average of 4-different orientations has resulted good classification rate and low error rate on all classifiers. The GLCM features on the proposed method outperformed the other existing methods. The proposed ULBPM achieved 85.85% classification rate with 0.08 of mean absolute error and 0.21 of root mean squared error (average of all classifiers).

Table 1: Classification table of ULBPM.

Texture name	Classifiers	Classification rate	Mean absolute error	Root mean squared error
Pressed Cork	NaïveBayes	56.48	0.17	0.39
	MLP	95.97	0.02	0.1
	Ibk	97.76	0.01	0.09
	J48	92.51	0.03	0.16
Herrigbone weave	NaïveBayes	57.38	0.17	0.39
	MLP	94.97	0.03	0.12
	Ibk	96.64	0.01	0.11
	J48	92.96	0.03	0.16
Grass lawn	NaïveBayes	56.98	0.17	0.39
	MLP	94.63	0.02	0.12
	Ibk	96.64	0.01	0.11
	J48	93.29	0.03	0.15
Wood Grain	NaïveBayes	54.3	0.18	0.4
	MLP	96.08	0.02	0.11
	Ibk	97.98	0.01	0.08
	J48	92.62	0.03	0.16
Pig Skin	NaïveBayes	60.55	0.16	0.37
	MLP	95.19	0.02	0.11
	Ibk	97.87	0.01	0.09
	J48	92.4	0.03	0.16
Water	NaïveBayes	61.23	0.21	0.45
	MLP	95.65	0.14	0.18
	Ibk	96.68	0.21	0.32
	J48	93.65	0.20	0.40

ISSN: 1992-8645 www.jatit.org E-ISSN: 1817-3195

Table 2: Classification table of CDTM.

Texture name	Classifiers	Classification rate	Mean absolute error	Root mean squared error
Pressed Cork	NaïveBayes	78.65	0.21	0.46
	MLP	82.32	0.41	0.41
	Ibk	80.12	0.45	0.31
	J48	76.63	0.32	0.5
Herrigbone weave	NaïveBayes	74.6	0.23	0.53
	MLP	83.59	0.27	0.24
	Ibk	82.81	0.41	0.39
	J48	78.38	0.32	0.34
Grass lawn	NaïveBayes	72.65	0.31	0.45
	MLP	81.51	0.44	0.26
	Ibk	75.65	0.24	0.34
	J48	76.3	0.48	0.31
Wood Grain	NaïveBayes	74.47	0.46	0.42
	MLP	83.98	0.21	0.24
	Ibk	83.46	0.22	0.28
	J48	78.77	0.31	0.34
Pig Skin	NaïveBayes	73.32	0.48	0.51
	MLP	82.31	0.26	0.26
	Ibk	80.16	0.42	0.32
	J48	78.68	0.32	0.32
Water	NaïveBayes	74.36	0.59	0.61
	MLP	82.69	0.25	0.29
	Ibk	83.47	0.22	0.29
	J48	78.49	0.48	0.33

Table 3: Classification table of GLCM.

Texture name	Classifiers	Classification rate	Mean absolute error	Root mean squared error
Pressed Cork	NaïveBayes	56.32	0.52	0.54
	MLP	64.25	0.31	0.45
	Ibk	63.11	0.38	0.41
	J48	61.24	0.41	0.52
Herrigbone weave	NaïveBayes	63.01	0.31	0.42
	MLP	63.36	0.38	0.39
	Ibk	59.36	0.51	0.56
	J48	61.2	0.41	0.48
Grass lawn	NaïveBayes	64.21	0.25	0.46
	MLP	65.36	0.32	0.45
	Ibk	64.38	0.31	0.58
	J48	60.54	0.43	0.53
Wood Grain	NaïveBayes	66.32	0.31	0.48
	MLP	66.71	0.32	0.47
	Ibk	64.36	0.41	0.49
	J48	61.2	0.54	0.53
Pig Skin	NaïveBayes	60.12	0.5	0.59
	MLP	63.35	0.35	0.51
	Ibk	62.45	0.39	0.55
	J48	61.11	0.5	0.58
Water	NaïveBayes	59.64	0.53	0.62
	MLP	65.34	0.42	0.46
	Ibk	63.42	0.33	0.52
	J48	61.52	0.49	0.58

Table 4: Classification table of TS.

Texture name	Classifiers	Classification rate	Mean absolute error	Root mean squared error
Pressed Cork	NaïveBayes	50.23	0.71	0.62
	MLP	54.35	0.61	0.65
	Ibk	53.12	0.63	0.68
	J48	50.45	0.73	0.79
Herrigbone weave	NaïveBayes	54.65	0.62	0.71
	MLP	52.36	0.68	0.71
	Ibk	49.65	0.81	0.75
	J48	51.42	0.78	0.69
Grass lawn	NaïveBayes	53.68	0.65	0.69
	MLP	54.63	0.63	0.7
	Ibk	53.98	0.67	0.7
	J48	50.74	0.72	0.78
Wood Grain	NaïveBayes	55.68	0.66	0.7
	MLP	56.45	0.62	0.58
	Ibk	54.86	0.62	0.72
	J48	51.45	0.78	0.69
Pig Skin	NaïveBayes	50.86	0.71	0.77
	MLP	53.68	0.68	0.71
	Ibk	50.45	0.75	0.78
	J48	51.23	0.78	0.68
Water	NaïveBayes	58.68	0.56	0.57
	MLP	60.21	0.53	0.56
	Ibk	56.36	0.62	0.59
	J48	57.84	0.59	0.61

*MLP: Multilayer perceptron

Journal of Theoretical and Applied Information Technology
30th November 2016. Vol.93. No.2

ISSN: 1992-8645 www.jatit.org E-ISSN: 1817-3195

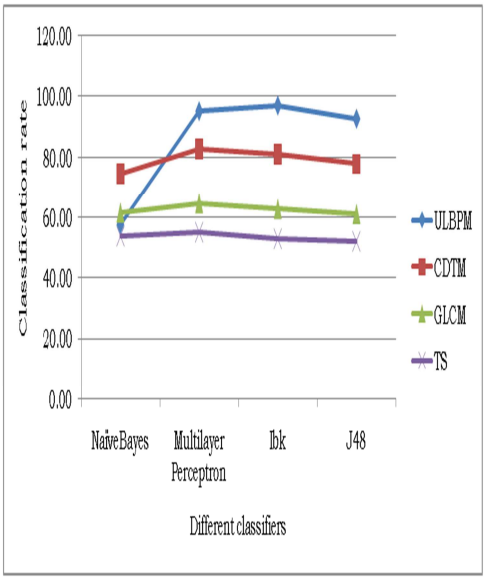

Fig.4: Average Texture Classification Rate Using Various Classifiers.

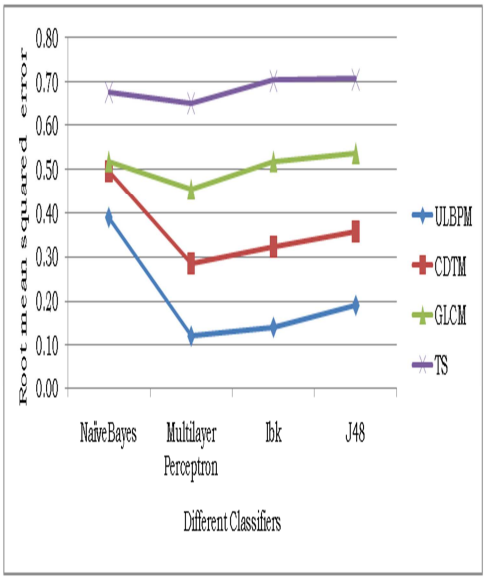

Fig. 6: Average Rate Of Mean Squared Error Of Classification

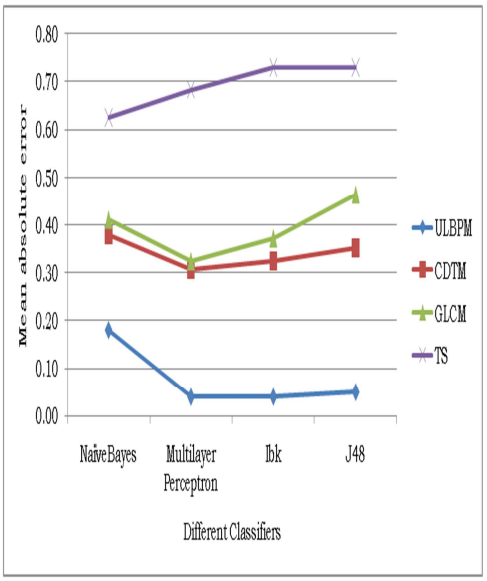

Fig. 5: Average Rate Of Mean Absolute Error Of Classification.

The multi-layer perceptron and Ibk classifiers have shown high classification rate on all three existing methods and the proposed method. However out of these two, Ibk exhibited a little high performance than multilayer perceptron. Out of the four classifiers naïve bayes classifiers has shown low classification rate on all the four methods (Fig.4)**.**The Fig.5 and Fig.6 shows the average rate of mean absolute error and mean squared error. The naive bayes achieved high error rate, indicates low performance.

4. CONCLUSIONS

This paper derived rotational invariant local features by considering the transitions form 1 to 0 or 0 to 1 on the LBP i.e. ULBP's. The proposed ULBPM treated all 197 NULBP codes **as** noisy codes and assigned a unique value zero to all NULBPs. This greatly reduced the overall dimension of ULBM and it is not proportional to the grey level range of texture and the size of the considered textures. The proposed ULBPM will have a fixed size of 59x59. The thirteen GLCM features on the proposed ULBPM classified the textures more efficiently than the other three existing methods i.e. GLCM, CDTM and TS. The present paper used four machine learning classifiers to derive classification, mean absolute error and mean squared error rate. Out of these four classifiers the Ibk and multilayer perceptron

ISSN: 1992-8645 www.jatit.org E-ISSN: 1817-3195

performed high classification rate and low error rates when compared to other two classifiers.

REFRENCES:

[1] Obulesu A, JS Kiran, VV Kumar, "Facial image retrieval based on local and regional features", IEEE, 2015 International Conference on Applied and Theoretical Computing and Communication Technology (iCATccT), pp: 841-846.

[2] Abdulrahman Al-Janobi, "Performance evaluation of cross-diagonal texture matrix method of texture analysis", Pattern Recognition 34 (2001) 171}, 180.

[3] Ahonen T., Hadid A., Pietikäinen M., "Face recognition with local binary patterns", 8th European Conf. on Computer Vision- 2004, Lecture Notes in Computer Science, Vol. 3021, pp. 469-481, 2004.

[4] Ahonen, T., Hadid, A., Pietikäinen, M., "Face description with local binary patterns: Application to face recognition", IEEE Trans. Pattern Anal. Mach. Intell. Vol. 28, no. 12, pp. 2037–2041, 2006.

[5] B.Eswar Reddy , P.Kiran Kumar Reddy and V.Vijaya Kumar, "Texture classification based on binary cross diagonal shape descriptor texture matrix (BCDSDTM)", ICGST-Graphics vision and image processing, (ICGST-GVIP), Vol.14, No.1, pp. 45-51, Aug-2014.

[6] Cardinaux F., Sanderson C., and Bengio S., "Face verification using adapted generative models", IEEE Conf. Automatic Face and Gesture Recognition, pp. 825-830, 2004.

[7] D.C. He, L. Wang, "Texture features based on texture spectrum", Pattern Recognition 24 (5) (1991) 391}399.

[8] Davis L.S., Johns S.A., Aggarwal J.K., "Texture analysis using generalized co-occurrence matrices", IEEE Trans. PAMI, Vol.1, no. 3, pp. 251-259, 1979.

[9] G S Murty , J Sasi Kiran , V.Vijaya Kumar, "Facial expression recognition based on features derived from the distinct LBP and GLCM", International journal of image, graphics and signal processing (IJIGSP), , Vol.2, No.1, pp. 68-77,2014,

[10] G. Zhao, M. Pietikaeinen, "Dynamic texture recognition using local binary patterns with an application to facial expressions", IEEE Transactions on Pattern Analysis and Machine Intelligence, Vol. 29, No. 6, 2007

[11] Haralick RM , Shanmugan K and Dinstein I, "Textural features for image classification", IEEE Trans. Sysr., Man., Cybern., Vol. SMC-3, no. 6, pp. 610-621, 1973.

[12] Haralick R.M., "Statistical and structural approaches to texture", Proceedings of the IEEE, Vol. 67, no. 5, pp. 786-804, 1979.

[13] iu, Guang-Hai, Lei Zhang, Ying-Kun Hou, Zuo-Yong Li, and Jing-Yu Yang, "Image retrieval based on multi-texton histogram", Pattern Recognition, Vol. 43, No. 7, 2010, pp. 2380-2389.

[14] J.S. Weszka, C.R. Dyer, A. Rosenfeld, "A comparative study of texture measures for terrain classification", IEEE Trans. Systems Man Cybernet 5 (1976) 269}285.

[15] Julesz B., "Experiments in the visual perception of textures", Scientific America, Vol. 232, pp. 34-43, 1975.

[16] K. Srinivasa Reddy, V.Vijaya Kumar, B.Eshwara reddy, "Face Recognition based on Texture Features using Local Ternary Patterns", I.J. Image, Graphics and Signal Processing, 2015, 10, 37-46 , ISSN: 2074-9082.

[17] K.Srinivasa Reddy , V. Venkata Krishna, V.Vijaya Kumar, "A Method for Facial Recognition Based On Local Features", International Journal of Mathematics and Computation, Vol.27; Issue No. 3, Year 2016, pp no. 98-109.

[18] Khouzani K.J., Hamid S.Z., "Radon transform orientation estimation for rotation invariant texture analysis", IEEE Trans. PAMI, Vol. 27, no. 6, pp. 1004-1008, 2005.

[19] L. Wang, D.C. He, "A new statistical approach for texture analysis", Photogrammetric Engng. Remote Sens. 56 (1)
(1990) 61}66.

[20] L.Liu, L.Zhao and P.Fieguth, "Extended local binary pattern for texture classification", Image and Vision Computing, 30(2) (2012) 86-99.

[21] M. Inen, M. Pietikäinen, A. Hadid, G. Zhao, and T. Ahonen, "Computer Vision Using Local Binary Patterns", vol. 40. New York, NY, USA: Springer- Verlag, 2011.

[22] MaÈenpaÈaÈ T., Ojala T., PietikaÈinen M., and Soriano M., "Robust texture classification by subsets of local binary patterns", Proc. 15th Int'l Conf. Pattern Recognition, vol.3, pp. 947-950, 2000.

[23] MaÈenpaÈaÈ T., PietikaÈinen M., and Ojala T., "Texture classification by multi-predicate

ISSN: 1992-8645 www.jatit.org E-ISSN: 1817-3195

local binary pattern operators", Proc. 15th Int'l Conf. Pattern Recognition, vol.3, pp.951-954, 2000.

[24] Matsuyama T., et al., "Structural analysis of natural textures by fourier transformation", Comput. Vision Graphics Images Process, Vol. 12, pp. 286-308, 1980.

[25] Maturana, D., Soto, A., Mery, D., "Face recognition with decision tree-based local binary patterns", Proc. Asian Conference on Computer Vision, Vol. 6495, pp. 618-629, 2011.

[26] Mu, Y.D., Yan, S.C., Liu, Y., Huang, T., Zhou, B.F., "Discriminative local binary patterns for human detection in personal album", Proc. IEEE Conference on Computer Vision and Pattern Recognition, pp. 1–8, 2008.

[27] Ojala T., PietikaÈinen M., and Harwood D., "A Comparative Study of Texture Measures with Classification Based on Feature Distributions"‖, Pattern Recognition, vol. 29, pp. 51-59, 1996.

[28] Ojala T., Pietikäinen M. and Mäenpää T., "Multiresolution gray-scale and rotation invariant texture classification with local binary patterns", IEEE Transactions on Pattern Analysis and Machine Intelligence, Vol. 24, no. 7, pp. 971-987, 2002.

[29] P. Brodatz, Textures: "A Photographic Album for Artists and Designers ".New York, NY, USA: Dover, 1999.

[30] R.F. Walker, "Adaptive Multi-scale Texture Analysis with Application to Automated Cytology", Ph.D. Thesis, The University of Queensland, 1997.

[31] S. H. Lee, J. Y. Choi, Y. M. Ro, and K. N. Plataniotis, "Local color vector binary patterns from multichannel face images for face recognition", IEEE Trans. Image Process., vol. 21, no. 4, pp. 2347–2353, Apr. 2012.

[32] S. Hussain and B. Triggs, "Visual recognition using local quantized patterns," in Proc. Eur. Conf. Comput. Vis., 2012, pp. 716–729.

[33] S. Liao, M. W. K. Law, and A. C. S. Chung, "Dominant local binary patterns for texture classification" IEEE Trans. Image Process., vol. 18,no. 5, pp. 1107–1118, May 2009.

[34] S. Wang, X. He, Q. Wu, and J. Yang, "Generalized local N-ary patterns for texture classification" in Proc. 10th IEEE Int. Conf. Adv. Video Signal Based Surveill., Aug. 2013, pp. 324–329.

[35] T. Ahonen, A. Hadid, and M. Pietikainen, "Face description with local binary patterns: Application to face recognition," IEEE Trans. Pattern Anal. Mach. Intell., vol. 28, no. 12, pp. 2037–2041, Dec. 2006.

[36] T.Ahonen, M.Pietikainen and A.Hadid, Face recognition with local binary pattern, ECCV, Springer, (2004) 469-481.

[37] T.Ojala, T.Maenpaa and M.Pietikainen. "Gray scale and rotation invariant texture classification with local binary pattern", Computer Vision, Springer, (2000) 404-420.

[38] Takala V., Ahonen T., and Pietik¨ainen M., "Block-based methods for image retrieval using local binary patterns", Proceedings of 14th SCIA, pp. 882-891, 2005.

[39] U Ravi Babu, V Vijaya Kumar ,J Sasi Kiran, "Texture analysis and classification based on fuzzy triangular grey level pattern and run length features", Global journal of computer science and technology graphics & vision (GJCST), Vol. 12, No. 15, pp. 17-23, 2012

[40] Unay. D., Octavian Soldea, Ahmet Ekin,Mujdat Cetin, Aytul Ercil, "Automatic Annotation of X-Ray Images: A Study on Attribute Selection", Medical Content-Based Retrieval for Clinical Decision Support, Lecture Notes in Computer Science, Volume 5853, pp. 97-10, 2010.

[41] V Vijaya Kumar, U S N Raju, K Chandra Sekaran, V V Krishna, "Employing long linear patterns for texture classification relying on wavelets", ICGST-Graphics, vision and image processing (ICGST-GVIP), Vol.8, No.5, pp. 13-21, Jan-2009.

[42] V. Vijaya Kumar, Jangala. Sasi Kiran ,G.S.Murthy, "Pattern based dimensionality reduction model for age classification", International journal of computer applications (IJCA), Vol.79, No.13, pp. 14-20, Oct-2013.

[43] V. Vijaya Kumar, P. Chandra Sekhar Reddy, B. Eswara Reddy, "New method for classification of age groups based on texture shape features", International journal imaging and robotics, Vol. 15, No.1, 2015

[44] V.Vijaya Kumar, K. Srinivasa Reddy V.Venkata krishyna, "Face Recognition using the Prominent LBP Model", International Journal of Applied Engineering Research (IJAER), ISSN: 1087-1090, 10(2), 2015, pp: 4373-4384.

[45] Vijaya Kumar, V., Eswar Reddy, B. et al. (2007). "An innovative technique of texture, classification and comparison based on long

ISSN: 1992-8645 www.jatit.org E-ISSN: 1817-3195

linear patterns". Journal of Computer Science, Science Publications, vol. 3(8), pp.633-638.

[46] Vijaya Kumar, V., Eswar Reddy, B., et al. (2008). "Classification of Textures by Avoiding Complex Patterns", Journal of Com. Science, vol. 4(2), pp.133-138

[47] X. Qi, R. Xiao, C.-C. Li, Y. Qiao, J. Guo, and X. Tang, "Pairwise rotation invariant co-occurrence local binary pattern," IEEE Trans. Pattern Anal. Mach. Intell., vol. 36, no. 11, pp. 2199–2213, Nov. 2014.

[48] X. Tan and B. Triggs, "Enhanced local texture feature sets for face recognition under difficult lighting conditions," in Proc. Anal. Modeling Faces Gestures, vol. 4778. 2007, pp. 168–182.

[49] Yung-Kaun Chan, Chin-Chen Chang, "Image matching using run-length feature", Pattern Recognition Letters, Vol. 22, no. 5, pp. 447-455, 2001.

[50] Z. Guo, L. Zhang, and D. Zhang, "A completed modeling of local binary pattern operator for texture classification," IEEE Trans. Image Process., vol. 9, no. 16, pp. 1657–1663, Jun. 2010.